

Molecular Dynamics and Experimental Study of Conformation Change of Poly(N-isopropylacrylamide)-hydrogels in Water

Jonathan Walter^a, Viktor Ermatchkov^a, Jadran Vrabec^b, Hans Hasse^{a,*}

^a*Laboratory of Engineering Thermodynamics, University of Kaiserslautern,
Kaiserslautern, Germany*

^b*Thermodynamics and Energy Technology, University of Paderborn, Paderborn,
Germany*

Abstract

The conformation change of Poly(N-isopropylacrylamide) (PNIPAAm) hydrogel as a function of temperature is studied both experimentally and by molecular simulation. The experiments show a theta-temperature of approximately 305 K and a width of the transition region of approximately 20 K, independent of the amount of cross-linker. The conformation change of the hydrogel is caused by a conformation change of the single polymer chains in its backbone. The latter was studied by massively parallel molecular dynamics simulations with GROMACS 4. Different force fields for describing the hydrogel backbone (GROMOS-87, GROMOS-96 53A6, and OPLS-AA) as well as the water molecule (TIP4P and SPC/E) were investigated. In the simulations the mean radius of gyration of the polymer chains was monitored.

*Corresponding author: Hans Hasse

Technische Universität Kaiserslautern, Lehrstuhl für Thermodynamik, Erwin-Schrödinger-Straße 44, 67663 Kaiserslautern, Germany, *phone* +49 631 205 3464, *fax* +49 631 205 3835

Email address: `hans.hasse@mv.uni-kl.de` (Hans Hasse)

URL: `thermo.mv.uni-kl.de` (Hans Hasse)

Two force field combinations (GROMOS-96 53A6 + TIP4P and OPLS-AA + SPC/E) yield the conformation change upon variation of the temperature. The results for OPLS-AA + SPC/E are in fair agreement with the experimental results.

Keywords:

PNIPAAm, hydrogel, polymer, swelling, conformation change, molecular dynamics, force field, temperature

1. Introduction

Hydrogels are three-dimensional hydrophilic polymer networks. Their most characteristic property is their swelling in aqueous solutions by absorbing the solvent, which is influenced by various factors. Hydrogels can be used in many applications. Superabsorbers such as in diapers [1] and contact lenses [2] are well established applications of hydrogels. But also applications like in drug delivery systems [3], tissue engineering [4], micro actuators [5] and epicardial restraint therapies [6] are discussed. To fully exploit the potential of hydrogels in all these applications, it is important to understand, describe and predict their swelling behaviour.

The hydrogel which is studied in the present work is built up of poly(N-isopropylacrylamide) (PNIPAAm) cross-linked with N,N'-methylenebisacrylamide (MBA). PNIPAAm is one of the most extensively studied hydrogels in the scientific literature and is mainly used in bioengineering applications [7]. The degree of swelling in equilibrium of PNIPAAm is significantly influenced by many factors [8–12]. On the one hand, the swelling depends on the structure of the hydrogel itself, like the type of the monomer, but also the

amount and type of cross-linker and of co-monomers. On the other hand, the environment conditions like temperature, type of solvent, solvent composition, salt concentration or pH-value of the solvent influence the swelling. Varying these factors, the hydrogel typically shows a region where the hydrogel is swollen and a region where it is collapsed. In between those two regions lies the region of conformation transition. The solvent composition or temperature, which is characteristic for that transition, is often labeled with Θ (Θ -solvent and Θ -temperature). Çaykara et al. [12] measured the degree of swelling of PNIPAAm as a function of the temperature in pure water and found a Θ -temperature for PNIPAAm hydrogel of approximately 305 K, which is the same as the lower critical solution temperature (LCST) of PNIPAAm polymer in pure water [13]. The degree of swelling depends on the amount of cross-linker and in some cases on the used co-monomer. A higher amount of cross-linker leads to a lower degree of swelling. However, the Θ -conditions are typically only weakly dependent on the amount of cross-linker. Therefore, the Θ -conditions mainly depend on the environmental factors and the nature of the polymer chain.

For the quantitative description of the swelling of hydrogels, various types of models are used [14]. Only two are briefly discussed here. In the model of Maurer and Prausnitz [15], the thermodynamic equilibrium between the solvent phase and the hydrogel phase is modelled. The hydrogel phase is modelled as a polymer solution with elastic properties. After determining the model parameters from experimental data, the swelling of the hydrogel can be described quantitatively and the swelling of the same hydrogel with varying amounts of cross-linker can be predicted. But it is not possible to quantita-

tively predict the swelling of other hydrogels or its dependence on other factors. Wallmersperger and Ballhause used a chemo-electro-mechanical model in finite element simulations of hydrogels [16, 17]. With this method, they simulated the influence of electric and mechanical fields on the swelling of charged hydrogels in solutions containing ions.

With molecular simulation it should in principle be possible to predict the swelling of different hydrogels upon varying any environmental factor. Two levels of model detail are applied for molecular simulations of hydrogels: coarse-grained and atomistic models. The advantage of coarse-grained models, especially in combination with implicit solvents, is their comparatively low computational cost. Coarse-grained models were used to study conformations of model hydrogels, depending on the solvent [18] or the amount of ions in the solvent and the charges on the hydrogel [19, 20]. In these studies, it was observed that the hydrogel and the corresponding single polymer chain have similar conformations in good, bad and Θ -solvents: Independent of whether a polymer chain is part of a hydrogel or a single chain, it is collapsed in bad solvents and stretched in good solvents and the transition occurs roughly at the same conditions.

Atomistic simulations are computationally much more expensive than coarse-grained simulations, especially when the solvent is modelled explicitly. With atomistic simulations, the dynamic properties and the conformation of the solvent and the monomers of the hydrogels have been studied by several authors [21–25]. Longhi et al. [25] studied the single PNIPAAm polymer with a chain length of 50 monomers using the all-atom force field Amber [26] and TIP3P [27] for water. The single polymer chain was simulated at

temperatures of 300 and 310 K and different conformations in equilibrium were observed. These conformations are neither clearly stretched nor clearly collapsed, but in a state in between.

The hydrogel network has to be idealized for molecular simulation. The network typically is described as an ideal cubic or diamond structure and the hydrogel network is typically fixed at the edges of the simulation volume. The equilibrium of the hydrogel networks is then characterized via the osmotic pressure [19] or the chemical potential [28–30] between the hydrogel phase and the solvent phase, simulated in a second simulation volume. In these studies, the conformations of the chains in the network and the influence of the cross-linker on the swelling behaviour are investigated qualitatively. In the literature, predominantly model hydrogels were studied. Even for simulations of real hydrogels, the validation on the basis of experimental data was difficult or not attempted at all.

In this work, the swelling of PNIPAAm hydrogel is studied with atomistic molecular dynamics simulation and by experiment. The results from simulation and experiment are compared to study whether the swelling behaviour of hydrogels can be quantitatively predicted by molecular simulation.

Images of PNIPAAm hydrogels, which were taken in this work after freeze-drying with nitrogen by electron microscopy, show large voids and small holes in the hydrogel structure, cf. Figure 1 and Wang et al. [31]. Furthermore, only the amount of cross-linker added to the reacting solution in hydrogel synthesis is known, but it is very difficult, if not impossible, to obtain reliable data on the fraction of cross-linker that has really reacted and whether it is attached to all reactive sites. Hence, the detailed structure of hydrogels

remains unknown. The degree of swelling cannot be quantitatively predicted by molecular simulations at present. But it should be possible to quantitatively predict the Θ -conditions for a given hydrogel by molecular simulation, as they are not sensitive to the details of the structure discussed above. In particular, from experimental data and coarse-grained simulation, it is known that the amount of cross-linker typically has no significant influence on the Θ -conditions of the hydrogel [11, 12, 19, 20]. The Θ -transition can be understood by studying single PNIPAAm chains as it depends on the interactions between the single chain and the solvent. In the present work, therefore molecular simulations were performed for single chains in explicitly modelled solvent molecules for a real hydrogel. Namely, the temperature dependence of the swelling behaviour of PNIPAAm in pure water was studied. For investigating the influence of temperature only force fields for PNIPAAm and water are needed. This allows testing the used force fields for their applicability in studies of more complex situations like adding salt or using mixed solvents.

For the present study, different force fields from the literature developed mainly for biomolecules in solvents are used as published. No parameters were fitted. The results are compared to experimental data of the degree of swelling of PNIPAAm hydrogel in pure water as a function of the temperature.

In the literature, the temperature dependence of the degree of swelling has often been measured in dynamic experiments, which leads to a heating/cooling hysteresis in the degree of swelling of the hydrogel [31, 32]. These experiments do not yield the degree of swelling in equilibrium. Çaykara et al. [12]

investigated the degree of swelling of PNIPAAm hydrogel in pure water as a function of the temperature in equilibrium, but did only publish graphical results. Therefore, the temperature dependent degree of swelling of PNIPAAm hydrogel was investigated experimentally in the present work.

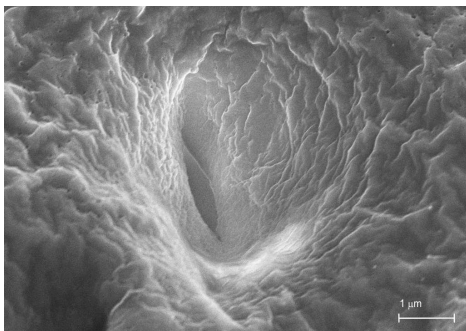


Figure 1: Image of freeze-dried swollen PNIPAAm hydrogel taken by electron microscopy in the present work.

2. Experimental Procedure and Results

The studied chemically cross-linked hydrogels were synthesized in the present work by polymerizing N-isopropylacrylamide (NIPAAm) and cross-linking it with N,N'-methylenebisacrylamide (MBA). The experimental method is only briefly described here. For a detailed description cf. Hüther and Maurer [9]. Polymerization and cross-linking were simultaneously carried out by free radical polymerization in oxygen-free, deionized water at 298 K under nitrogen atmosphere. The reactions were initiated by small amounts of ammonium peroxodisulfate (starter) and sodium disulfite (accelerator).

For the synthesis, the monomer NIPAAm (Aldrich, 97 %, CAS 2210-25-5), the cross-linking agent MBA (Fluka, 99 %, CAS 110-26-9), and the initiators

ammonium peroxodisulfate ((NH₄)₂S₂O₈) (Aldrich, 98 %, CAS 7727-54-0) and sodium disulfite (Na₂S₂O₅) (Fluka, 98 %, CAS 7681-57-4) were used without further purification. Oxygen-free, bi-distilled water was used for synthesis and for the swelling experiments. After synthesis, the hydrogel particles were thoroughly washed with deionized water and dried in a vacuum oven at room temperature.

In addition to the production process, the hydrogels are characterized by the following concentrations in the aqueous polymerization solution: Total mass fraction x_{gel}^m of polymerizable material

$$x_{gel}^m = \frac{m_{NIPAAm} + m_{MBA}}{m_{total}}, \quad (1)$$

mole fraction of cross-linking agent x_{MBA}^n

$$x_{MBA}^n = \frac{n_{MBA}}{n_{NIPAAm} + n_{MBA}}, \quad (2)$$

and mass fraction of the initiator x_s^m

$$x_s^m = \frac{m_s}{m_{total}}. \quad (3)$$

Here, m and n are the mass and mole number, respectively. The parameters for the three hydrogels synthesized in the present work are presented in Table 1.

For each swelling experiment, ten dried hydrogel particles were used. The amount of mass of the dried hydrogel particle was determined with a precision micro balance (type MX5, Mettler Toledo GmbH, Giessen, Germany) before pure water was added to the particles. The hydrogel in water was thermostated in an air oven (model ICP 600, Memmert, Schwabach, Germany) for approximately two weeks. For temperature measurement, a calibrated

Table 1: Characterization of the synthesized hydrogels: Total mass fraction x_{gel}^m of polymerizable material, mole fraction of cross-linking agent x_{MBA}^n and mass fraction of the initiator x_s^m .

Hydrogel	$x_{gel}^m / \text{g}\cdot\text{g}^{-1}$	$x_{MBA}^n / \text{mol}\cdot\text{mol}^{-1}$	$x_s^m / \text{g}\cdot\text{g}^{-1}$
1	0.0995	0.0498	$1.97\cdot 10^{-4}$
2	0.1000	0.0400	$2.04\cdot 10^{-4}$
3	0.1001	0.0200	$2.03\cdot 10^{-4}$

platinum resistance thermometer with an overall uncertainty of ± 0.1 K was used. After reaching equilibrium, the hydrogel particles were taken out of the water and the surface water was removed. The mass of the swollen particles was determined with the precision micro balance. The degree of swelling of each particle was calculated as the ratio of mass of the swollen hydrogel m_{gel} to the mass of the dry hydrogel $m_{gel}^{(dry)}$

$$q = \frac{m_{gel}}{m_{gel}^{(dry)}}. \quad (4)$$

For the ten experiments, the arithmetic mean and the standard deviation of the degree of swelling were calculated. The experiments were performed at different temperatures to determine the influence of the temperature on the degree of swelling. The experimental results are summarized in Table 2.

3. Discussion of Experimental Results

Figure 2 presents the experimental results for the degree of swelling of the three different hydrogels in water as a function of the temperature. The bars denote the standard deviations, which are mostly within the symbol size.

Table 2: Degree of swelling as a function of temperature for three different hydrogels in water (cf. Table 1). The numbers behind \pm denote the standard deviation.

Hydrogel 1		Hydrogel 2		Hydrogel 3	
$x_{gel}^m = 0.0498 \text{ g}\cdot\text{g}^{-1}$		$x_{gel}^m = 0.0400 \text{ g}\cdot\text{g}^{-1}$		$x_{gel}^m = 0.0200 \text{ g}\cdot\text{g}^{-1}$	
T	q	T	q	T	q
K	$\text{g}\cdot\text{g}^{-1}$	K	$\text{g}\cdot\text{g}^{-1}$	K	$\text{g}\cdot\text{g}^{-1}$
288.15	15.76 ± 0.17	288.15	16.52 ± 0.13	288.15	20.14 ± 0.18
293.15	14.73 ± 0.18	293.15	15.53 ± 0.28	293.15	18.87 ± 0.24
298.15	12.51 ± 0.27	298.15	13.50 ± 0.25	298.15	15.75 ± 0.46
303.15	9.77 ± 0.13	303.15	9.99 ± 0.28	303.15	12.38 ± 0.31
305.67	6.47 ± 0.22	305.67	6.70 ± 0.40	305.67	7.40 ± 0.13
305.75	6.66 ± 0.17	305.75	6.46 ± 0.22	305.76	7.43 ± 0.23
308.15	3.74 ± 0.18	308.15	3.24 ± 0.14	308.15	1.93 ± 0.10
313.15	1.55 ± 0.07	313.15	1.53 ± 0.03	313.15	1.52 ± 0.07
318.77	1.42 ± 0.05	318.78	1.50 ± 0.08	319.20	1.50 ± 0.06

The three hydrogels mainly differ in the degree of cross-linking (cf. Table 1). All hydrogels are swollen at low temperatures and collapsed at high temperatures. The Θ -temperature, defined here as temperature of the inflection point of $q(t)$, is approximately 305 K, which is in very good agreement with the measurements of Çaykara et al. [12] and the LCST of PNIPAAm polymer in pure water [13]. The width of the conformation transition region is approximately 20 K. The Θ -temperature does not depend on the amount of cross-linker. Therefore, it can be assumed that molecular simulation of the swelling behaviour of hydrogels on the basis of single chains is an appropriate method.

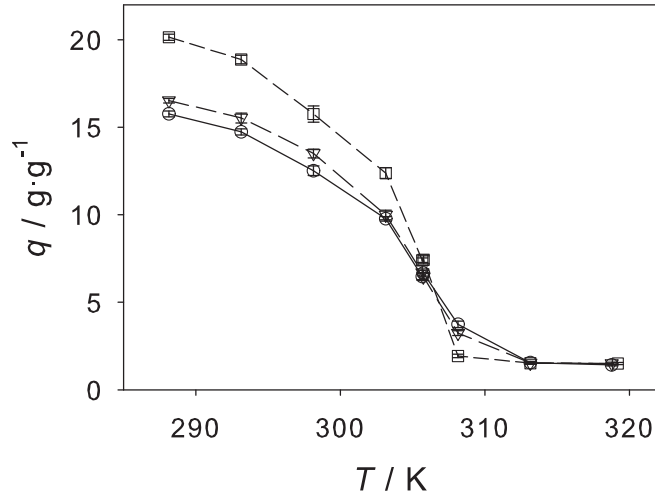


Figure 2: Degree of swelling of the PNIPAAm hydrogel 1 ($x_{gel}^m = 0.0498 \text{ g}\cdot\text{g}^{-1}$) ○, 2 ($x_{gel}^m = 0.0400 \text{ g}\cdot\text{g}^{-1}$) ▽, and 3 ($x_{gel}^m = 0.0200 \text{ g}\cdot\text{g}^{-1}$) □ as a function of temperature. Symbols: experimental data from this work, lines: guide for the eye. The error bars denote the standard deviation.

4. Force Fields

For the molecular dynamics simulations of PNIPAAm in water, the following force fields from the literature were used: The three force fields GROMOS-87 (G87) [33], GROMOS-96 53A6 (G53A6) [34, 35] and OPLS-AA (OPLS) [36, 37] were employed to describe PNIPAAm. They were combined with two models for water, namely SPC/E [38] and TIP4P [27]. G87 and G53A6 are united-atom force fields, OPLS is an all-atom force field. These force fields were mainly developed based on structural data of various larger molecules. For the development of the force fields OPLS and G53A6, additionally thermophysical data of pure liquids of small molecules like alcohols and amino acids was used. The Lennard-Jones (LJ) and point charge parameters of the PNIPAAm force fields are listed in Tables 3 and 4. The LJ-sites are characterized by the size parameter σ and the energy parameter ϵ . For the water models, the parameters are listed in Table 5. For the unlike LJ pair interaction, a geometric mean mixing rule for both σ and ϵ was used

$$\begin{aligned}\sigma_{ij} &= \sqrt{\sigma_i \cdot \sigma_j}, \\ \epsilon_{ij} &= \sqrt{\epsilon_i \cdot \epsilon_j}.\end{aligned}\tag{5}$$

For the intramolecular interactions, the method of the 1-4 interactions was employed [39]. Thereby, the interactions between a given atom and its first and second neighbour are only modeled by the bond and the angle term. Interactions between the atom and its third neighbour are calculated by the dihedral, the Coulomb interaction and the LJ term. The last two terms are reduced by a scaling factor, where the value of it depends on the force field. All other intramolecular interactions are modeled with the unmodified

Table 3: Lennard-Jones parameters (σ and ϵ) and point charge magnitude (q_{el}) of the PNIPAAm force fields G87 [33] and G53A6 [34, 35], where e is the elementary charge.

site	G87			G53A6		
	σ / nm	ϵ / kJ·mol ⁻¹	q_{el} / e	σ / nm	ϵ / kJ·mol ⁻¹	q_{el} / e
C	0.3361	0.4058	0.38	0.3581	0.2774	0.45
O	0.2626	1.7245	-0.38	0.2760	1.2791	-0.45
N	0.2976	0.8767	-0.28	0.3136	0.6398	-0.31
H	-	-	0.28	-	-	0.31
CH	0.4232	0.5441	-	0.5019	0.0949	-
CH ₂	0.3965	0.5856	-	0.4070	0.4105	-
CH ₃	0.3786	0.7533	-	0.3748	0.8672	-

Coulomb interaction and LJ term.

A peculiarity of the parameters of the three PNIPAAm force fields should be noted. The LJ parameters of CH for the force field G53A6 is not in line with the other LJ parameters in these force fields. The value for σ is much higher and the value for ϵ is much lower. A reason for this might be that the LJ parameters of this force field was developed in the C6 and C12 form, in which σ and ϵ are combined

$$\begin{aligned}
 \text{C6} &= 4\epsilon\sigma^6, \\
 \text{C12} &= 4\epsilon\sigma^{12}.
 \end{aligned}
 \tag{6}$$

Further, the difference between an all-atom and an united-atom model can be seen in comparison of the ϵ values of CH_x for the three force fields.

Table 4: Lennard-Jones parameters (σ and ϵ) and point charge magnitude (q_{el}) of the PNIPAAm force field OPLS [36, 37], where e is the elementary charge.

site	OPLS		
	σ / nm	ϵ / kJ·mol ⁻¹	q_{el} / e
C	0.375	0.4393	0.50
O	0.296	0.8786	-0.50
N	0.325	0.7113	-0.50
H	-	-	0.30
CH(-N)	0.350	0.2761	0.14
CH	0.350	0.2761	-0.06
CH ₂	0.350	0.2761	-0.12
CH ₃	0.350	0.2761	-0.18
H in CH _x	-	-	0.06

Table 5: Force field parameters for water. Lennard-Jones parameters (σ and ϵ), point charge magnitude of the oxygen site (q_{el}), distance O-H (L), angle H-O-H (ϕ) and distance O-point charge (l) of the SPC/E [38] and TIP4P [27] models, where e is the elementary charge.

force field	σ / nm	ϵ / kJ·mol ⁻¹	q_{el} (O) / e	L / nm	ϕ / deg	l / nm
SPC/E	0.3166	0.6502	-0.8476	0.10000	109.47	0.000
TIP4P	0.3154	0.6485	-1.0400	0.09572	104.52	0.015

5. Simulation Methods

Molecular simulations of PNIPAAm single chains were carried out with versions 4.0.x of the GROMACS simulation package [40, 41]. The GROMACS code is optimized for single processors and also for massively parallel simulations. It was developed for the simulation of large molecules in solutions. The simulations were performed on the high performance computer HP XC 4000 at the Steinbuch Centre for Computing in Karlsruhe (Germany), which is equipped with Opteron 2.6 GHz Dual Core processors.

In order to study the applicability of the force fields, in a first step simulations with all six combinations of the PNIPAAm + water force fields were performed at temperatures of 280 and 360 K. These temperatures are well below and well above the experimental Θ -temperature of PNIPAAm in water, while the lower temperature is still above the freezing point of the water models. In equilibrium at the lower temperature, the single chain should be in a stretched conformation, at the higher temperature it should be collapsed. The simulations were started both from stretched and from collapsed initial conformations to simulate the process of collapsing and stretching of the PNIPAAm chains. After having identified suitable force field combinations, simulations at temperatures between 280 and 360 K were performed, namely at 290, 300, 310, 320 and 340 K. These allow to obtain the Θ -temperature and the width of the transition region.

Prior to these simulations, some preliminary studies were performed in which the chain length, the initial configuration and the thermostat were varied.

For equilibration, the single PNIPAAm chains in water were simulated in the isobaric-isothermal ensemble over 1 to $5 \cdot 10^7$ timesteps. The pressure

was specified to be 1 bar and was controlled by the Berendsen barostat [42], the timestep was 1 fs for all simulations. Newton’s equations of motion were numerically solved with the leap-frog integrator [43]. For the long-range electrostatic interactions, particle mesh Ewald [44] with a grid spacing of 0.12 nm and an interpolation order of four was used. A cutoff radius of $r_c = 1.5$ nm was assumed for all interactions. After equilibration, 2 to $4 \cdot 10^7$ production time steps were carried out with constant simulation parameters. Note that the production steps include the conformation transition as well as the simulation of the equilibrium.

In order to analyze the results, the radius of gyration R_g was calculated

$$R_g = \left(\frac{\sum_i ||\mathbf{r}_i||^2 m_i}{\sum_i m_i} \right)^{1/2}, \quad (7)$$

which characterizes the degree of stretching of the single chain, where m_i is the mass of site i and $||\mathbf{r}_i||$ is the norm of the vector from site i to the center of mass of the single chain. The radius of gyration in equilibrium was calculated as the arithmetic mean over the last $5 \cdot 10^6$ time steps of the simulation together with its standard deviation. In addition, the potential energy between polymer and solvent as well as between polymer and polymer was calculated. For the visualization of the results the open source program VMD [45] was used.

6. Preliminary Studies

6.1. Thermostat

In this work, the influence of the temperature on the conformation of PNIPAAm chains was examined. Therefore, it is important to use a suitable

thermostat. Thus two thermostats Nosé-Hoover [46] and velocity-rescale [47] were tested and their damping parameters τ_T were varied. This study was carried out with a system of one 30 monomer PNIPAAm chain and 14,482 water molecules with the force field combination OPLS + SPC/E, starting from an equilibrated configuration. From these simulations, the average temperature T and its standard deviation σ_T were calculated.

Both thermostats yield the same average temperature and the same standard deviation σ_T of about 1.3 K for damping parameters between 0.1 and 1. The velocity-rescale thermostat was chosen with a damping parameter of 0.5, because of its simplicity and stability [39].

6.2. Initial Configuration

In order to simulate stretching and collapsing of PNIPAAm chains, both collapsed and stretched initial configurations were needed. For generating stretched initial configurations an energy minimization was performed with a maximum force of 5 kJ/(mol·nm) for the interactions inside the chain. The resulting conformation and radius of gyration of the isolated single chain are similar to the stretched conformation of single chains in equilibrium in water (cf. Figure 3).

Collapsed initial conformations can not straightforwardly be obtained from energy minimization. To obtain such initial conformations at different degrees of collapse of the single chain, a simulation of the PNIPAAm chain in water was performed at a temperature of 360 K, starting from a stretched initial conformation. During this simulation the chain collapses. From the trajectory of this simulation, starting configurations with different degrees of

collapse were selected. In Figure 3 typical stretched and collapsed conformations of the single chain are shown.

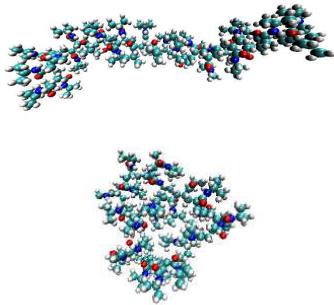


Figure 3: Typical stretched (top) and collapsed (bottom) conformation of a PNIPAAm chain with $N = 30$ monomers in equilibrium with water (water molecules not shown).

6.3. Chain length

The length of the single chain in simulation has an influence on the results and on the computational cost. Shorter chains need less simulation time, but too short chains will not yield significant conformation transitions. In a preliminary study, single PNIPAAm chains with 15, 30, 50 and 75 monomers were simulated in water at 360 K, starting from a stretched initial conformation. In these simulations a single chain should collapse.

Figure 4 shows the results plotted over the simulation time. To compare the radius of gyration of chains with different number of monomers, the radius of gyration R_g is normalized by the radius of gyration of the stretched single chain in equilibrium R_0 . The value R_0 was obtained from simulations at 280 K, where the single chain is stretched in equilibrium. It can be seen that the chains with more than 15 monomers collapse and remain collapsed

in equilibrium. Only the chain consisting of 15 monomers shows no significant changes in conformation. The radius of gyration fluctuates between two values over the hole simulation time. The second observation is that longer chains need more time for the conformation transition (approximately 3, 5 and 7.5 ns for 30, 50 and 75 monomers, respectively). Thus simulations of longer chains need more computation time because of the system size and they also demand more simulation time steps.

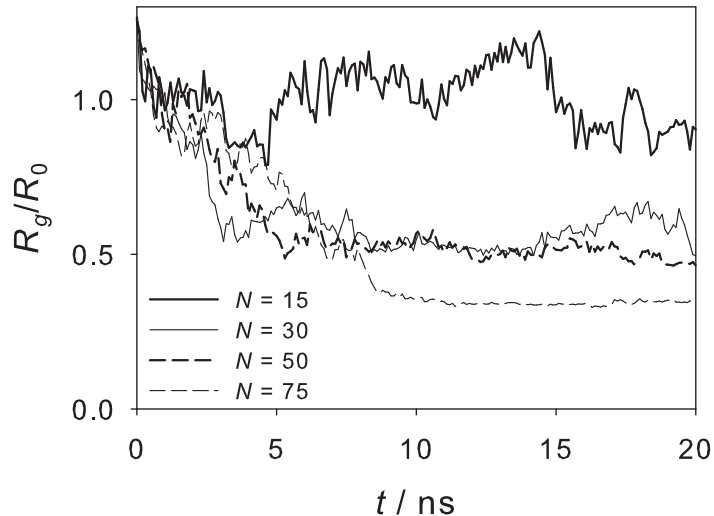


Figure 4: Reduced radius of gyration of PNIPAAm single chains of different chain lengths (N : number of monomers) in water as a function of time. The simulations start in a stretched initial configuration at 360 K for the force field combination OPLS + SPC/E.

In order to obtain significant results with a reasonable computational effort, single chains with 30 monomers were simulated in the present study. This leads to computation times between one and three days on 128 cores of the mentioned PC-cluster.

7. Results and discussion

7.1. Applicability of different force fields

Figures 5 and 6 present the simulation results for PNIPAAm for the different force field combinations at 280 and 360 K, which are below and above the Θ -temperature, respectively. The radius of gyration R_g is plotted over the simulation time t , starting from a stretched initial conformation. In Figure 5, the simulation results at 280 K are presented. At this temperature, the single chain should in equilibrium be in a stretched conformation. Only the two force field combinations OPLS + SPC/E and G53A6 + TIP4P clearly remain in a stretched configuration. Three other force field combinations show a collapse of the single chain (G53A6 + SPC/E, G87 + TIP4P and G87 + SPC/E). For the force field combination OPLS + TIP4P the state in equilibrium is difficult to define.

Figure 6 shows the simulation results at 360 K. At that temperature, the chains should collapse, when starting from a stretched initial configuration. All force field combinations show a collapse for this temperature. The only noticeable difference in these simulations is that the conformation transition occurs after a distinctly longer simulation for the force field combination G53A6 + TIP4P time than for the other combinations. This simulation was continued for another 20 ns. The single chain stays in a collapsed conformation (not shown here).

The two force field combinations that are able to yield both the stretched and the collapsed configuration of the single chain are OPLS + SPC/E and G53A6 + TIP4P. Note that the two force field combinations that predict the correct conformations at 280 and 360 K are not recommended by their

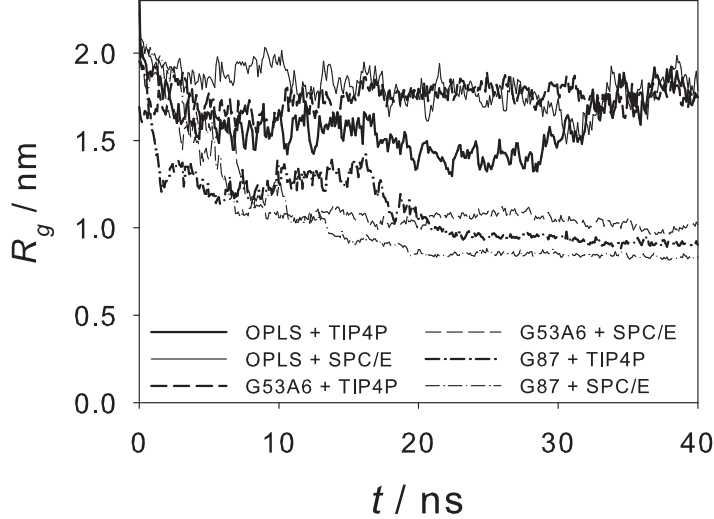


Figure 5: Radius of gyration R_g of a PNIPAAm chain of 30 monomers in 14,482 water molecules over simulation time t for different force field combinations at 280 K.

developers. The OPLS force field was developed for TIP4P water and G53A6 for SPC water.

Furthermore, it was studied whether the force field combinations are able to show conformation transitions in both directions. For this test, only the force field combinations OPLS + SPC/E and G53A6 + TIP4P were used. The results of these simulations are presented in Figures 7 and 8, where the radius of gyration is again plotted over simulation time. Figure 7 shows the simulation results of single PNIPAAm chains with the force field combination OPLS + SPC/E. The curves at the top and at the bottom represent the simulations starting from the stretched initial configuration at temperatures of 280 and 360 K, respectively. For the three other simulations, starting conformations (1, 2, 3) from the simulation at 360 K at different times were

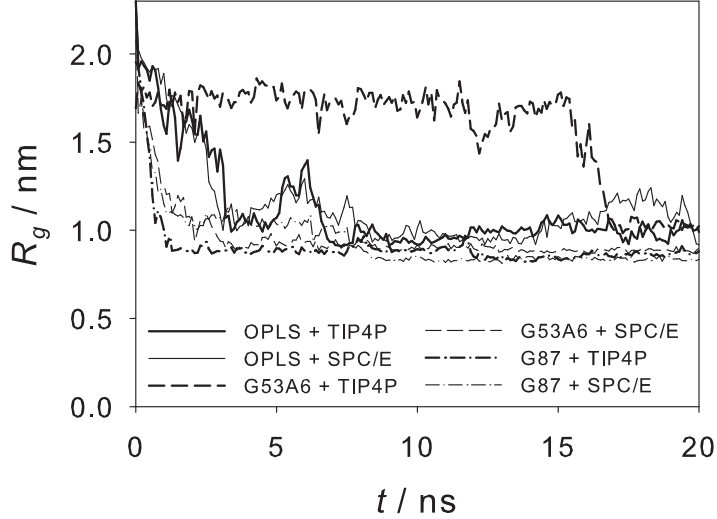


Figure 6: Radius of gyration R_g of a PNIPAAm chain of 30 monomers in 14,482 water molecules over simulation time t for different force field combinations at 360 K.

chosen and the temperature was switched 280 K. The simulations with the starting conformations 1 and 2 show the conformation transition from the collapsed to the stretched single chain. The simulation with the starting conformation 3 shows that the chain, once completely collapsed, did not unfold again during simulation time. The result from this study is that the conformation transition from the collapsed to the stretched conformation can be simulated with the force field combination OPLS + SPC/E, but this conformation transition is slower than the collapse.

Results for the same type of simulations for the force field combination G53A6 + TIP4P can be seen in Figure 8. For this force field combination, the conformation transition is faster in both directions.

The comparison of the two force field combinations OPLS + SPC/E and

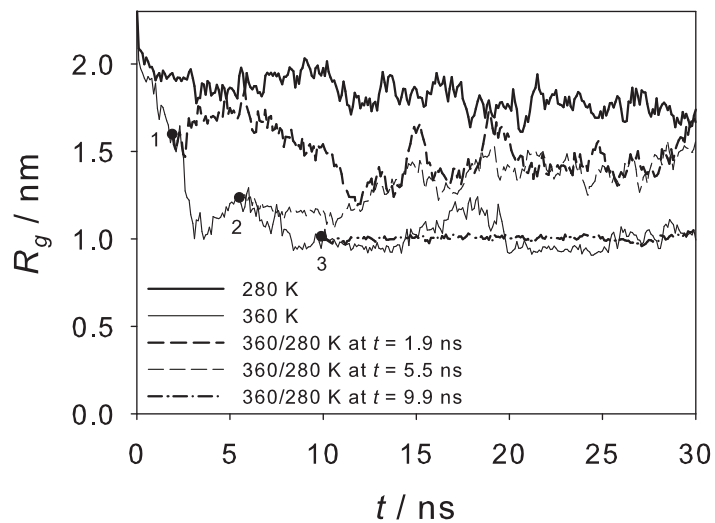


Figure 7: Radius of gyration R_g of a PNIPAAm chain of 30 monomers in 14,482 water molecules over simulation time t for the force field combination OPLS + SPC/E. The upper and the lower curves are for the stretched initial conformation at 280 and 360 K, respectively. For the three other simulations, starting conformations from the simulation at 360 K at different times • (1, 2, 3) were selected and the temperature was switched 280 K.

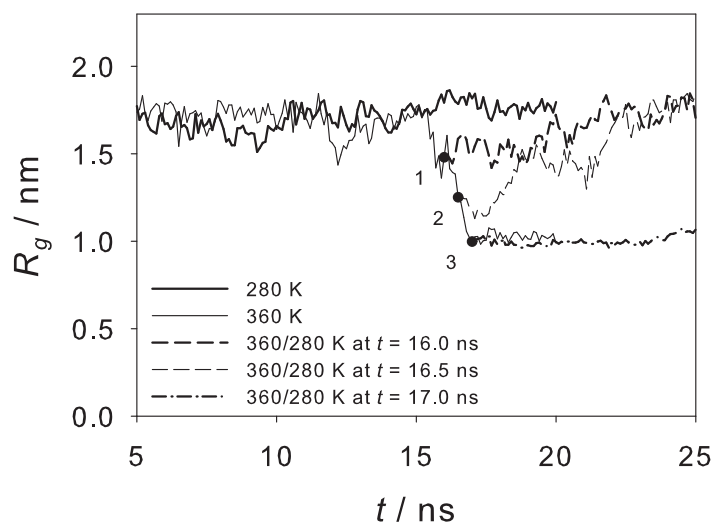


Figure 8: Radius of gyration R_g of a PNIPAAm chain of 30 monomers in 14,482 water molecules over simulation time t for the force field combination G53A6 + TIP4P. The upper and the lower curves are for the stretched initial conformation at 280 and 360 K, respectively. For the three other simulations, starting conformations from the simulation at 360 K at different times • (1, 2, 3) were selected and the temperature was switched 280 K.

G53A6 + TIP4P shows that both force field combinations are able to predict the conformation transition in both directions. At the same time, both force field combinations exhibit a radius of gyration for the PNIPAAm chain of 30 monomers in equilibrium in water of approximately 1.8 nm for 280 K and approximately 1.0 nm for 360 K.

7.2. Determination of the Θ -temperature

For the successful force field combinations OPLS + TIP4P and G53A6 + SPC/E, simulations at temperatures between 280 and 370 K were carried out in order to determine the radius of gyration in equilibrium as a function of temperature and to use that information for determining the Θ -temperature and the width of the transition region. The simulation results are shown in Figures 9 and 10, where the radius of gyration is again plotted over the simulation time. The simulations were performed starting from the same stretched initial configuration. Figures 9 and 10 only show the simulation results up to 20 ns as data up to that time were taken in all cases. However, several simulations were carried out longer, in order to make sure that the conformation reached after 20 ns does not change anymore. The maximal simulation time was 40 ns. The results for times larger than 20 ns are not shown as they provided no essential new information on the conformation. The radius of gyration in equilibrium was determined from a time average over the last 5 ns of the run. For the force field combination OPLS + SPC/E (Figure 9) there are many stable conformations in between the stretched and the collapsed conformation for different temperatures. In contrast to this, the force field combination G53A6 + TIP4P (Figure 10) only yields two stable conformations for the different temperatures, a stretched and a collapsed

conformation. The sharp transition occurs approximately at 353 K.

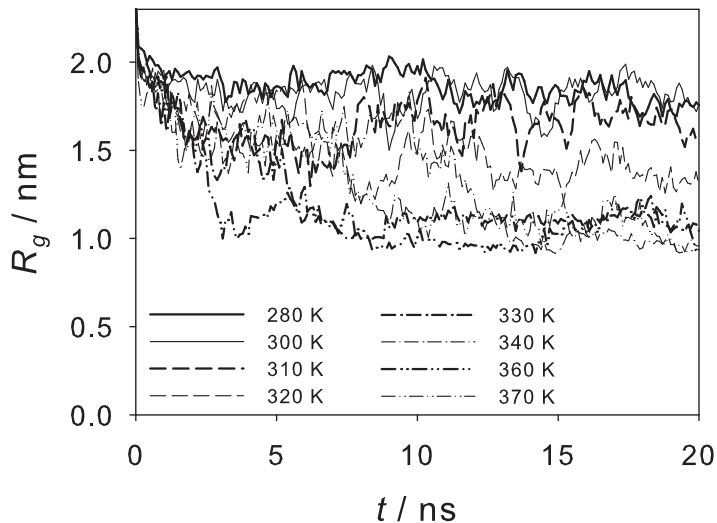


Figure 9: Radius of gyration R_g of a PNIPAAm chain of 30 monomers in 14,482 water molecules over simulation time t for different temperatures for the force field combination OPLS + SPC/E.

Figure 11 and Tables 6 and 7 present the results for the radius of gyration as a function of the temperature for the two force field combinations OPLS + SPC/E and G53A6 + TIP4P. The filled triangles in Figure 11 and Table 6 represent the results for OPLS + SPC/E. For temperatures below 300 K, the single chain is stretched, for temperatures above 340 K, it is collapsed. The Θ -temperature is approximately 320 K. The width of the transition region is approximately 40 K.

The filled circles in Figure 11 and Table 7 represent the results for the same study with the force field combination G53A6 + TIP4P. These results differ from those observed for the force field combination OPLS + SPC/E, as there

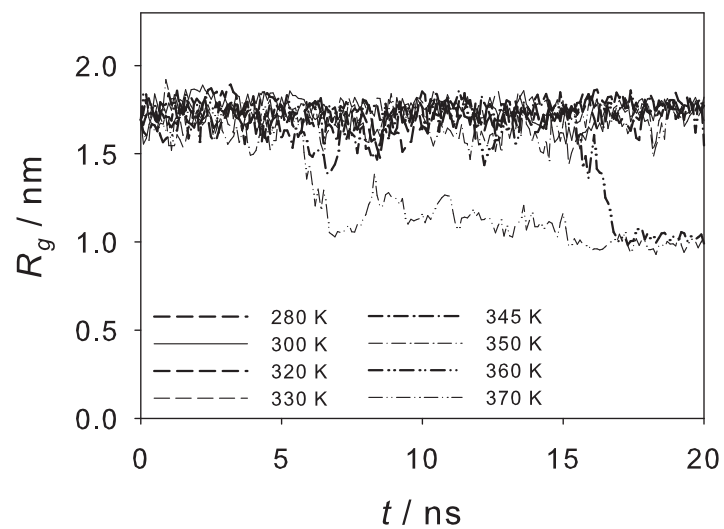


Figure 10: Radius of gyration R_g of a PNIPAAm chain of 30 monomers in 14,482 water molecules over simulation time t for different temperatures for the force field combination G53A6 + TIP4P.

is a sharp conformation transition between the stretched and the collapsed confirmation. For temperatures below 350 K, the single chain is stretched, for temperatures above 355 K, it is collapsed. Therefore the Θ -temperature for this model is at approximately 353 K and the width of the transition region is not larger than 5 K.

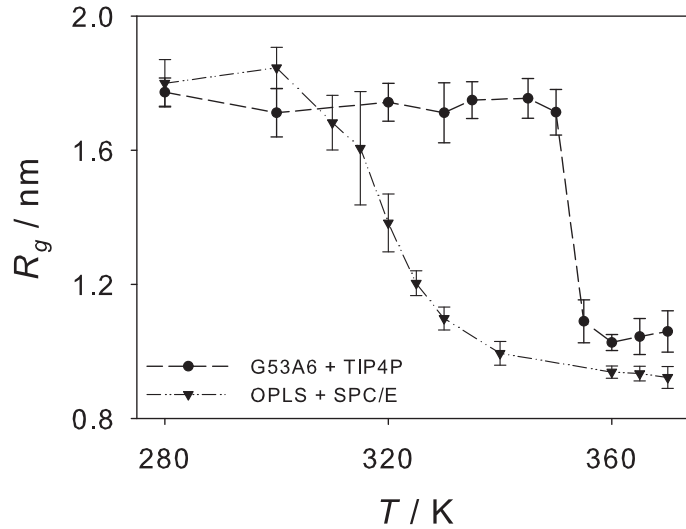


Figure 11: Radius of gyration R_g of a PNIPAAm chain of 30 monomers in 14,482 water molecules in equilibrium over temperature T for the force field combination OPLS + SPC/E and G53A6 + TIP4P. The error bars indicate the standard deviation.

Obviously, the results for the force field combination OPLS + SPC/E (filled triangles in Figure 11) are in better agreement with the experimental data (Figure 2) than those for the force field combination G53A6 + TIP4P (filled circles in Figure 11). With the force field combination OPLS + SPC/E, qualitatively correct results were achieved. The main difference between the experimental data and the prediction by molecular simulation is that the

Table 6: Radius of gyration R_g of a PNIPAAm chain of 30 monomers in 14,482 water molecules in equilibrium over temperature T for the force field combination OPLS + SPC/E. The numbers behind \pm denote the standard deviation.

T / K	R_g / nm
280	1.80 ± 0.07
300	1.85 ± 0.06
310	1.68 ± 0.08
315	1.61 ± 0.17
320	1.38 ± 0.09
325	1.20 ± 0.04
330	1.10 ± 0.03
340	0.99 ± 0.04
360	0.94 ± 0.02
365	0.93 ± 0.02
370	0.92 ± 0.03

Table 7: Radius of gyration R_g of a PNIPAAm chain of 30 monomers in 14,482 water molecules in equilibrium over temperature T for the force field combination G53A6 + TIP4P. The numbers behind \pm denote the standard deviation.

T / K	R_g / nm
280	1.77 ± 0.04
300	1.71 ± 0.07
320	1.74 ± 0.06
330	1.71 ± 0.09
335	1.75 ± 0.06
345	1.76 ± 0.06
350	1.71 ± 0.07
355	1.09 ± 0.06
360	1.03 ± 0.02
365	1.04 ± 0.05
370	1.06 ± 0.06

Θ -temperature is about 15 K higher and the width of the transition region is overestimated in the molecular simulation. In summary, this is an unexpectedly favourable agreement between the prediction by molecular simulation and the experimental data, especially when considering that the force fields were not trained on such type of data and no adjustments were made.

For a more detailed insight, the potential energy from simulation was studied. Due to the fact that pairwise additive force fields were used, the total potential energy U can be split into three parts

$$U = U_{PP} + U_{WW} + U_{PW}, \quad (8)$$

where U_{PP} is the potential energy of the polymer-polymer interactions, U_{WW} the potential energy of the water-water interactions, and U_{PW} the potential energy of the polymer-water interactions. The contribution of the water-water interactions does not significantly depend on the conformation of the polymer chain. But it can be expected that the ratio U_{PW}/U_{PP} will be strongly affected by the conformation. Namely, high numbers of that ratio can be expected for the stretched configuration, whereas low numbers can be expected for the collapsed conformation. Results are shown in Figure 12 for the two force field combinations OPLS + SPC/E and G53A6 + TIP4P. These results are the sum of the LJ and Coulomb potentials measured within the cutoff radius. The ratio U_{PW}/U_{PP} is plotted as a function of simulation time at 280 and 360 K for a PNIPAAm chain of 30 monomers in water. By comparing Figure 12 with Figures 7 and 8, it can clearly be seen that the chain collapse is associated with a significant decrease of U_{PW}/U_{PP} . From a comparison of the two force field combinations, it can be seen that the stretched conformation has a higher value of U_{PW}/U_{PP} for the force field

combination G53A6 + TIP4P. The ratio U_{PW}/U_{PP} is for both temperatures higher than for the force field combination OPLS + SPC/E. This probably leads to the late conformation transition from the stretched to the collapsed conformation at 360 K for the force field combination G53A6 + TIP4P.

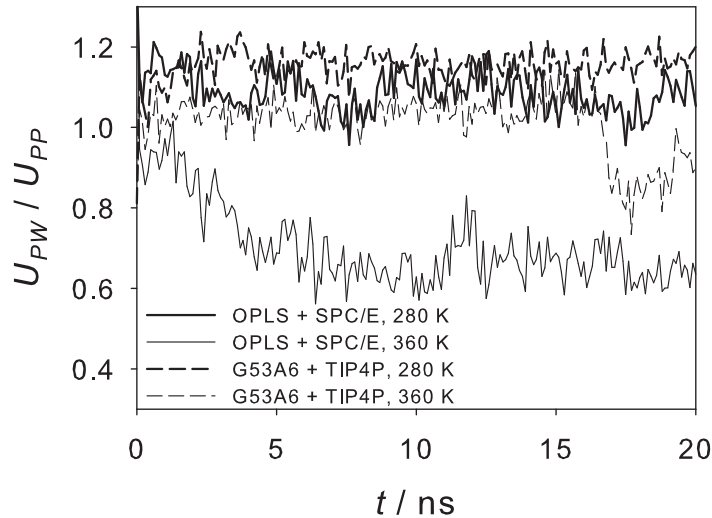


Figure 12: Ratio of the potential energy of the polymer-water interaction U_{PW} and polymer-polymer interaction U_{PP} as a function of simulation time t . The collapse of the chains is associated with a decrease of U_{PW}/U_{PP} (cf. Figures 7 and 8). The simulations were performed with a chain PNIPAAm of 30 monomers in 14,482 water molecules.

8. Conclusion

The temperature dependence of swelling of PNIPAAm hydrogels in pure water was studied both experimentally and by molecular simulation. The experiments show a Θ -temperature of approximately 305 K and a width of the transition region of approximately 20 K. Furthermore, it was observed

that the Θ -temperature is independent of the amount of cross-linker in the hydrogel.

It was found that it is possible to study the conformation transition of PNIPAAm hydrogel by molecular simulation of the single polymer chain. The force field combinations G53A6 + TIP4P and OPLS + SPC/E yield the stretched and the collapsed conformations as well as the conformation transition. Four other studied force field combinations yield only the collapsed conformation. With the force field combination OPLS + SPC/E, it is possible to qualitatively predict the swelling of the hydrogel as a function of temperature. A Θ -temperature for the PNIPAAm single chain in pure water of approximately 320 K and a width of the conformation region of approximately 40 K was predicted. For the force field combination G53A6 + TIP4P, a sharp transition at approximately 353 ± 2 K was observed.

Molecular simulation is a useful tool for predicting conformation transitions of real hydrogels. Accurate quantitative results can be expected, if suitable force fields are available.

Abbreviations

G53A6	GROMOS-96 53A6
G87	GROMOS-87
LJ	Lennard-Jones
MBA	N,N'-methylenebisacrylamide
NIPAAm	N-isopropylacrylamide
OPLS	OPLS-AA
PNIPAAm	Poly(N-isopropylacrylamide)

List of symbols

$C6$	modified LJ parameter
$C12$	modified LJ parameter
l	distance between oxygen site and charge of the molecular water models
L	distance between oxygen and hydrogen site of the molecular water models
m	mass
n	molar number
N	number of monomers
q	degree of swelling
q_{el}	charge
r	distance
r_c	cutoff radius
R_g	radius of gyration
R_0	radius of gyration for a stretched chain in equilibrium
t	simulation time
T	temperature
U	potential energy
x^m	mass fraction
x^n	mole fraction
ϵ	energy parameter of the Lennard-Jones potential
σ	size parameter of the

	Lennard-Jones potential
σ_T	standard deviation
τ_T	damping parameter, thermostat
ϕ	angle between hydrogen, oxygen and hydrogen site of the molecular water models

Indices

<i>gel</i>	polymerizable material
<i>i</i>	site index
<i>j</i>	site index
<i>MBA</i>	cross-linker (MBA)
<i>NIPAAm</i>	monomer (NIPAAm)
<i>P</i>	polymer
<i>s</i>	starter
<i>total</i>	synthesis solution
<i>W</i>	water

9. Acknowledgement

We gratefully thank the German Research Foundation (DFG) for funding support in the Collaborative Research Centre 716. The computer simulations were performed on the high performance computer HP XC 4000 from the Steinbuch Centre for Computing in Karlsruhe (Germany) under the project acronym LAMO. For the picture of the hydrogel the electron microscope of the NanoBio Center at the University of Kaiserslautern (Germany) was used.

This work was carried out under the auspices of the Boltzman-Zuse Society for Computational Molecular Engineering.

10. References

References

- [1] A. El-Rehim, *Radiat. Phys. Chem.* 74 (2005) 111–117.
- [2] V. N. Pavlyuchenko, O. V. Sorochinskaya, S. S. Ivanchev, S. Y. Khaikin, V. A. Trounov, V. T. Lebedev, E. A. Sosnov, I. V. Gofman, *Polym. Adv. Technol.* 20 (2009) 367–377.
- [3] N. Peppas, P. Bures, W. Leobandung, H. Ichikawa, *Eur. J. Pharm. Biopharm.* 50 (2000) 27–46.
- [4] B. V. Slaughter, S. S. Khurshid, O. Z. Fisher, A. Khademhosseini, N. A. Peppas, *Adv. Mater.* 21 (2009) 3307–3329.
- [5] H. van der Linden, W. Olthuis, P. Bergveld, *Lab Chip* 4 (2004) 619–624.
- [6] K. L. Fujimoto, Z. Ma, D. M. Nelson, R. Hashizume, J. Guan, K. Tobita, W. R. Wagner, *Biomaterials* 30 (2009) 4357–4368.
- [7] Z. M. O. Rzaev, S. Dincer, E. Piskin, *Prog. Polym. Sci.* 32 (2007) 534–595.
- [8] A. Hüther, B. Schäfer, X. Xu, G. Maurer, *Phys. Chem. Chem. Phys.* 4 (2002) 835–844.
- [9] A. Hüther, G. Maurer, *Fluid Phase Equilib.* 226 (2004) 321–332.

- [10] A. Hüther, X. Xu, G. Maurer, *Fluid Phase Equilib.* 219 (2004) 231–244.
- [11] A. Hüther, X. Xu, G. Maurer, *Fluid Phase Equilib.* 240 (2006) 186–196.
- [12] T. Caykara, S. Kiper, G. Demirel, *J. Appl. Polym. Sci.* 101 (2006) 1756–1762.
- [13] M. Heskins, J. E. Guillet, *J. Macromol. Sci., Part A* 8 (1968) 1441–1455.
- [14] S. Wu, H. Li, J. P. Chen, K. Y. Lam, *Macromol. Theory Simul.* 13 (2004) 13–29.
- [15] G. Maurer, J. M. Prausnitz, *Fluid Phase Equilib.* 115 (1996) 113–133.
- [16] D. Ballhause, T. Wallmersperger, *Smart Mater. Struct.* 17 (2008) 045011.
- [17] T. Wallmersperger, D. Ballhause, *Smart Mater. Struct.* 17 (2008) 045012.
- [18] A. V. Lyulin, B. Dünweg, O. V. Borisov, A. A. Darinskii, *Macromolecules* 32 (1999) 3264–3278.
- [19] B. A. Mann, K. Kremer, C. Holm, *Macromol. Symp.* 237 (2006) 90–107.
- [20] H. J. Limbach, C. Holm, *J. Phys. Chem. B* 107 (2003) 8041–8055.
- [21] E. Chiessi, F. Cavaliere, G. Paradossi, *J. Phys. Chem. B* 109 (2005) 8091–8096.
- [22] E. Chiessi, F. Cavaliere, G. Paradossi, *J. Phys. Chem. B* 111 (2007) 2820–2827.

- [23] Y. Tamai, H. Tanaka, *Chem. Phys. Lett.* 285 (1998) 127–132.
- [24] T. Tönsing, C. Oldiges, *Phys. Chem. Chem. Phys.* 3 (2001) 5542–5549.
- [25] G. Longhi, F. Lebon, S. Abbate, S. L. Fornili, *Chem. Phys. Lett.* 386 (2004) 123–127.
- [26] W. D. Cornell, P. Cieplak, C. I. Bayley, I. R. Gould, J. Kenneth M. Merz, D. M. Ferguson, D. C. Spellmeyer, T. Fox, J. W. Caldwell, P. A. Kollman, *J. Am. Chem. Soc.* 117 (1995) 5179–5197.
- [27] W. L. Jorgensen, J. Chandrasekhar, J. D. Madura, R. W. Impey, M. L. Klein, *J. Chem. Phys.* 79 (1983) 926–935.
- [28] B. Knopp, U. W. Suter, *Macromolecules* 30 (1997) 6114–6119.
- [29] Z.-Y. Lu, R. Hentschke, *Phys. Rev. E* 65 (2002) 041807.
- [30] Z.-Y. Lu, R. Hentschke, *Phys. Rev. E* 66 (2002) 041803.
- [31] B. Wang, X.-D. Xub, Z.-C. Wang, S.-X. Cheng, X.-Z. Zhang, R.-X. Zhuo, *Colloids Surf., B* 64 (2008) 34–41.
- [32] M. Shibayama, T. Tanaka, C. C. Han, *J. Chem. Phys.* 97 (1992) 6842–6854.
- [33] W. F. van Gunsteren, H. J. C. Berendsen, *Gromos-87 manual*, Biomos BV Nijenborgh 4, 9747 AG Groningen, The Netherlands (1987).
- [34] W. F. van Gunsteren, S. Billeter, A. Eising, P. Hünenberger, P. Krüger, A. Mark, W. Scott, I. Tironi, *Biomolecular Simulation: The Gromos 96*

- Manual and User Guide, vdf Hochschulverlag AG an der ETH Zürich, Zürich, Switzerland, 1996.
- [35] C. Oostenbrink, A. Villa, A. E. Mark, W. F. van Gunsteren, *J. Comput. Chem.* 25 (2004) 1656–1676.
- [36] W. L. Jorgensen, J. Tirado-Rives, *J. Am. Chem. Soc.* 110 (1988) 6.
- [37] W. L. Jorgensen, D. S. Maxwell, J. Tirado-Rives, *J. Am. Chem. Soc.* 118 (1996) 11225–11236.
- [38] H. J. C. Berendsen, J. R. Grigera, T. P. Straatsma, *J. Phys. Chem.* 91 (1987) 6269–6271.
- [39] D. van der Spoel, E. Lindahl, B. Hess, A. R. van Buuren, E. Apol, P. J. Meulenhoff, D. P. Tieleman, A. L. T. M. Sijbers, K. A. Feenstra, R. van Drunen, H. J. C. Berendsen, *Gromacs User Manual version 3.3*, www.gromacs.org (2005).
- [40] D. van der Spoel, E. Lindahl, B. Hess, G. Groenhof, A. E. Mark, H. J. C. Berendsen, *J. Comput. Chem.* 26 (2005) 1701–1718.
- [41] B. Hess, C. Kutzner, D. van der Spoel, E. Lindahl, *J. Chem. Theory Comput.* 4 (2008) 435–447.
- [42] H. J. C. Berendsen, J. P. M. Postma, W. F. van Gunsteren, A. DiNola, J. R. Haak, *J. Chem. Phys.* 81 (1984) 3684–3690.
- [43] R. W. Hockney, S. P. Goel, J. W. Eastwood, *J. Comput. Phys.* 14 (1974) 148–158.

- [44] U. Essmann, L. Perera, M. L. Berkowitz, T. Darden, H. Lee, L. G. Pedersen, *J. Chem. Phys.* 103 (1995) 8577–8592.
- [45] W. Humphrey, A. Dalke, K. Schulten, *J. Mol. Graphics* 14 (1996) 33–38.
- [46] W. G. Hoover, *Phys. Rev. A* 31 (1985) 1695–1697.
- [47] G. Bussi, D. Donadio, M. Parrinello, *J. Chem. Phys.* 126 (2007) 014101.

Manuscript with Highlighted Changes

[Click here to download Supplementary Material: paper_walter_changes.pdf](#)